J. Physiol. (1979). **291**, *pp.* 117–141
With 1 plate and 9 text-figures
Printed in Great Britain

SIZE, SCATTER AND COVERAGE OF GANGLION CELL RECEPTIVE FIELD CENTRES IN THE CAT RETINA

BY L. PEICHL* AND H. WÄSSLE*
Physiologische Psychologie, Universität Konstanz, D-7750 Konstanz, W. Germany

(*Received 4 September 1978*)

SUMMARY

1. Receptive field centre sizes of brisk-sustained (X) and brisk-transient (Y) ganglion cells of the cat retina were assessed by three different methods: small spot mapping, area threshold method and spatial resolution.

2. Centre sizes of brisk-sustained (X) cells increased from 20′ in the central area to about 70′ at an eccentricity of 4·5 mm, centre sizes of brisk-transient (Y) cells from 50′ in the central area to about 140′ at 5 mm eccentricity.

3. The scatter of centre sizes at one retinal location was measured by recording as many ganglion cells as possible in one cat in a small field of retina. The centre sizes of the individual classes were homogeneous and exhibited only a small amount of scatter.

4. The coverage of the retina by the different ganglion cell classes was assessed from their density and their receptive field centre area. At every retinal location the receptive field centres of seven to twenty brisk-sustained (X) cells and of three to six brisk-transient (Y) cells were found to overlap. Sluggish concentric and non-concentric cells taken together have a coverage factor of about 60.

INTRODUCTION

The receptive fields of the majority of ganglion cells in the cat retina are concentrically organized into centres with antagonistic surrounds (Kuffler, 1953, Rodieck & Stone, 1965; Levick, 1975). It has been suggested that the physiological dimensions of the centre should be defined by the dendritic field size of a ganglion cell and the surround should be of a more varied extent, organized by the amacrine cells and their synapses (Gallego, 1965; Brown & Major, 1966; Dowling & Boycott, 1966; Creutzfeldt, Sakmann, Scheich & Korn, 1970). Detailed data are now available for the dendritic field dimensions of the ganglion cells (Boycott & Wässle, 1974) but the published physiologically determined receptive field centre sizes differ for different authors (Cleland & Levick, 1974*a*; Hammond, 1974; Stone & Fukuda, 1974). Thus the exact structural relationships of concentrically organized receptive fields remain unclear.

* Present address: Friedrich Miescher Labor der Max Planck Gesellschaft, Spemannstr. 37, D-7400 Tübingen, W. Germany.

0022-3751/79/3430-0714 $01.50 © 1979 The Physiological Society

A possible reason for the discrepancies between the physiological results is that the exact dimensions of receptive field centres are dependent on the methods of measurement employed. Therefore in the present paper three different methods (small spot mapping, area threshold, spatial resolution) are used to assess the dimensions of receptive field centres as accurately as possible, which then can be correlated with the anatomical data.

The spatial transfer characteristics of retinal ganglion cells are closely correlated with their receptive field dimensions (Enroth-Cugell & Robson, 1966). If the receptive fields of a particular ganglion cell class at one retinal location have a large range of sizes this would have the effect that the spatial information is transferred with different bandpass characteristics, that is by different 'channels' (Campbell, Cooper & Enroth-Cugell, 1969). If on the other hand the receptive fields at a particular retinal location all have the same sizes, only one bandpass would be present. The actual scatter of receptive field centre sizes will be tested in the present paper by recording and analysing in a single cat at a particular retinal position as many ganglion cells as possible. This avoids the additional scatter which is introduced by pooling the results from different animals and different retinal locations.

At each point of the retina the receptive fields of several ganglion cells overlap. Contingent on their physiological type they transmit different messages to the visual centres of the brain concerning the local light distribution on the retina. This rather peripheral separation of the visual information into parallel pathways has been investigated within the past decade in detail in cat retinal ganglion cells (Enroth-Cugell & Robson, 1966; Cleland, Dubin & Levick, 1971; Stone & Hoffmann, 1972; Cleland, Levick & Sanderson, 1973; Cleland & Levick, 1974*a*, *b*; Stone & Fukuda, 1974). It is an open question, whether the receptive field centres of all physiological classes of ganglion cells cover every point of the retina, or whether the cells of some of the classes are so sparsely distributed that only patches of the retina are covered by those cells. This question can be answered if the receptive field centre sizes and densities of the particular classes are known. The densities can be assessed accurately only from histology and we were able to identify quantitatively the different cell classes from retinal whole mount preparations. Combination of those results with the receptive field centre measurements can give the desired information about the coverage of the retina with the different ganglion cell classes.

The present paper considers only brisk-sustained (X) and brisk-transient (Y) cells because the number of our quantitative receptive field data on sluggish-concentric and non-concentric cells was not sufficient to allow a similar analysis of this heterogeneous population.

METHODS

Experiments were performed on eleven adult cats of either sex (2·5–4·5 kg). Anaesthesia was induced with 2–4 % halothane (Hoechst) in a 2:1 mixture of nitrous oxide and carbogen and maintained during surgery with 1–2 % halothane. The vagosympathetic trunk was severed on the left side (for improved ocular stability) and a tracheal cannula inserted. Throughout the period of data collection the animal was maintained on a mixture of 70 % nitrous oxide, 28·5 % oxygen and 1·5 % carbon dioxide given by artificial ventilation at 33 strokes/min with a stroke volume determined by the formula $\delta = 16{\cdot}6 \times W^{0{\cdot}77}$, where δ is the stroke volume in ml., W is the weight of the cat in kg (Cleland & Levick, 1974*a*). The percentage of nitrous oxide used has

been shown to maintain a suitable level of light anaesthesia in cats (Venes, Collins & Taub, 1971). Whenever necessary, halothane was used in addition to nitrous oxide. Penicillin and streptomycin (Cortexilar-PS, Grünenthal) were given I.M. in a dose of 250,000 u. daily. Muscular relaxation was obtained by I.V. infusion of gallamine triethiodide (Flaxedil) at 5 mg/kg.hr and D-tubocurarine (Curarin-Asta) at 0·3–0·5 mg/kg.hr. The infusion was given at a rate of 3 ml./hr in isotonic glucose solution. Experiments normally lasted 3–4 days.

Intraocular recording

The animal's head was fixed in a stereotaxic head holder (Wässle, 1975). A metal ring with attached micromanipulator foot plate was fixed to the left eyeball encircling the globe just behind the limbus (Cleland, Dubin & Levick, 1971). Tungsten-in-glass electrodes (Levick, 1972) were introduced into the eye *via* a small cannula and extracellular recordings from ganglion cells or their axons were obtained. The electrode was connected to a Grass P 15 preamplifier (filter-bandpass 0·3–3 kHz, amplification × 1000). The action potentials were displayed on an oscilloscope and fed into an audiomonitor with clipping facility.

Electrical stimulation

Shielded bipolar stimulating electrodes (1 mm bare tips, 1 mm tip separation) were stereotaxically inserted through small craniotomy openings at H.-C. anterior 10·0, lateral 9·0 into both optic tracts. Stimulus pulses were derived from a Devices isolator, pulse durations were 50 μsec, pulse amplitudes were up to 80 V.

Optics of the eye and visual landmarks

The corneae were protected by opaque plastic contact lenses with a transparent round centre of 4 mm diameter (artificial pupil). Atropine (1 %) eye-drops were employed to dilate the pupil and paralyse accommodation and Neosynephrine (1 %) drops were used to retract lids and nictitating membrane on the left side. The refraction of the eye was measured with an eye refractometer (Rodenstock) and corrected for the screen distance by spectacle glasses. In all experiments the optic disk and the ophthalmoscopically estimated position of the central area were back-projected on to a frontal tangent screen with a firmly fixed hand ophthalmoscope (Heine) as described by Fernald & Chase (1971). The screen was located at a distance of 172 cm in front of the animal's eyes so that 1° of visual angle subtended 3 cm on the screen. Throughout the experiments the optical quality of the eye was checked with the ophthalmoscope. As soon as the eye media became cloudy the experiments were terminated.

Optical stimulation

An optical stimulator was positioned behind the body of the cat and projected *via* a mirror onto the tangent screen. The mirror was centred in a precise goniometer and by setting the screws of the goniometer a light spot on the screen could be positioned with a precision of about 0·5 mm, which subtends 1′ of arc for the cat's viewing distance. The stimulator was equipped with a noiseless shutter, the light source was a d.c. driven halogen bulb (150 W, 24 V). A set of apertures was used to project onto the tangent screen accurately concentric circular light spots with diameters ranging in small steps from 3 to 340′. By means of neutral density filters (Schott NG 4) the light spots projected onto the screen could be varied in intensity over 3 log units in steps of 0·04 log units. The background illumination on the screen was 13 cd/m^2, the brightest light spots were 30 cd/m^2 (background + stimulus).

Procedure

The electrode was advanced towards the retina and action potentials from a single unit were recorded. The receptive field of a unit was first sought on the tangent screen; contrast targets of various sizes (black or white discs mounted on handles) were moved about until the region was found over which the maintained discharge could be strongly disturbed. A centre of symmetry was marked by making passes across the receptive field in various directions. The size of the

smallest disk having any effect and the size and speed producing an optimum response gave clues for the type of receptive field. The antidromic latency of the unit to single pulses (50 μsec duration, 1/sec repetition rate), the threshold of the electrical stimulus eliciting an antidromic spike and the optic tract from which the unit could be activated were measured and gave additional clues for the classification of the unit (Cleland & Levick, 1974*a*, *b*). The exact dimensions of the receptive field centres were measured by three successive methods.

1. *Small spot mapping.* A light spot of 17 cd/m^2 added to a uniform background of 13 cd/m^2 was flashed on and off at a rate of 1 Hz at different positions within the receptive field of a unit. The spot size was about 20 % of the presumed receptive field centre diameter. The response of the unit was carefully observed on an audiomonitor. While the spot was in the centre of the receptive field the unit normally responded with vigorous discharges; when the spot approached the border of the receptive field centre the centre type of response ceased; on moving the spot further out a weak surround type of response could be elicited. The position where the centre response had decreased so that it could be heard on only 50 % of trials was taken to be the border of the receptive field centre. The centre of the stimulus spot at this place was marked on the screen. The determination was repeated at several positions around the centre until a smooth curve could be drawn through the points. The region so defined was usually circular, occasionally rather elliptical (e.g. Text-fig. 3*B*); therefore an average diameter was derived by calculating the geometric mean of the major and minor axes of the outline. The centre of that circle was marked on the screen as the position of the unit.

2. *Area threshold measurement.* Light spots of increasing diameters were centred precisely at the centre of the receptive field and flashed on and off at a rate of 1 Hz. The response of the cell was carefully observed and the light intensity was gradually changed by inserting different neutral density filters. The intensity at which a centre type of response could be detected by ear in just 50 % of the trials was recorded as the threshold of the cell for that particular spot size. Mostly the threshold for about 10 well spaced spot sizes was determined. Finally the threshold for flashing the light on and off on the whole screen was determined (Ganzfeld).

3. *Spatial resolution.* Grating stimuli consisting of mounted photographic prints of parallel, equal width, black and white stripes were moved slowly across the receptive field on the screen. A cell normally responded very clearly with a modulated discharge to each period of the grating, but when the spatial frequency of the grating was increased above a certain value the cell no longer gave a modulated discharge. The spatial frequency at which a modulated discharge could just be detected by ear was taken as the resolution limit of the cell. The range of spatial frequencies tested was 0·9–24 c/deg and the ratio between successive spatial frequencies was 1·30. For elliptical fields the resolution along the long and short axes were separately determined and the mean was taken as the cell's resolution. Jerky movement of the grating mostly elicited a 'periphery effect' (McIlwain, 1964; Levick, Oyster & Davies, 1965) or 'shift effect' (Fischer, Krüger & Droll, 1975) and this was carefully differentiated from the modulated discharge during the smooth movement.

Testing a unit by all three methods normally required about 1 hr of careful measurements. In a successful experiment some twenty cells could be completely analysed.

Histology

In order to confirm the retinal positions of recording areas histologically, the following procedure was routinely used. At the end of an experiment a retinal lesion was produced by passing direct current (1·5 μA for 7 sec, electrode negative) through the recording electrode. The lesion was placed at the recording site of a brisk-sustained (X) unit. Because this cell class has small receptive field centres, the position of the lesion could be accurately plotted on the screen. The animal was then deeply anaesthetized with Nembutal (Abbott), the eye excised and a retinal whole mount preparation was made and stained with cresyl violet as described in detail by Wässle, Levick & Cleland (1975). The retinal lesion can be identified in the histological preparation (Cleland, Levick & Wässle, 1975) and allows one to correlate the retinal landmarks back-projected onto the screen with the corresponding structures in the whole mount (see Pl. 1). In that way the topographical position of each recorded cell could be determined with an accuracy of $\pm$ 100 μm.

RESULTS

1. *Classification of units*

In eleven adult cats sixty-nine ganglion cells of the brisk-transient (Y) type and ninety-seven ganglion cells of the brisk-sustained (X) type were analysed in detail and are included in the results. Altogether many more cells were recorded, but partly they were lost during recording and the analysis could not be completed, partly they belonged to other physiological classes. Text-fig. 1 shows the topographical positions

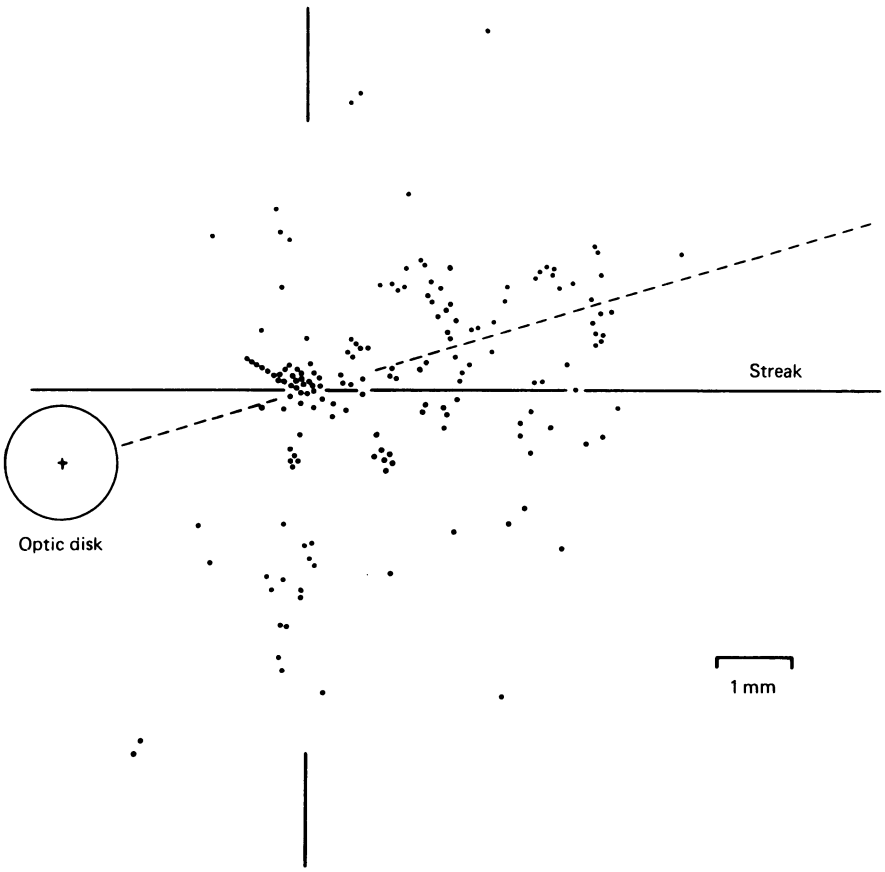

Text-fig. 1. Topographical positions of the recorded 166 ganglion cells on a schematic retina of the left eye. The central area would be at the intersection of the indicafed horizontal and vertical meridians. The dashed line connecting the optic disk and the central area is tilted 16° from the horizontal arm of higher ganglion cell density ('streak).

of the 166 ganglion cells on the retina. Most of the cells were recorded in the temporal retina because the histological results of Boycott & Wässle (1974) which we are going to compare are also from that part of the retina. In accordance with the description of Cleland & Levick (1974*a*, *b*) the application of a battery of tests (response to standing

contrasts, behaviour to grating patterns, sensitivity to size, speed and contrast of disk targets, antidromic latency) permitted the classification of brisk-sustained (X) and brisk-transient (Y) units. Text-fig. 2 demonstrates some typical characteristics of those two cell classes. Text-fig. 2*A* shows a spike recording and a smoothed pen

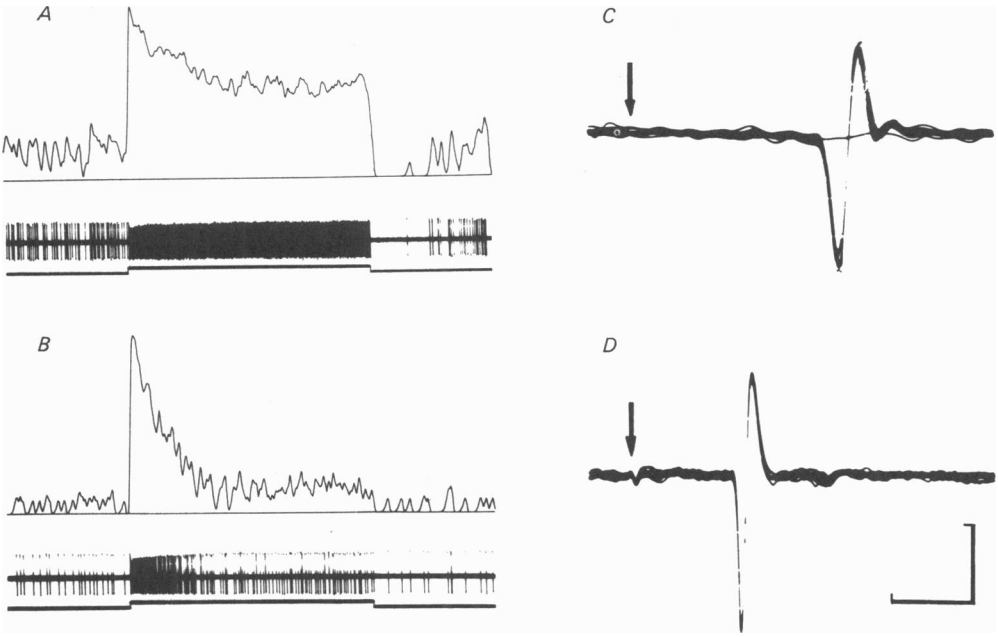

Text-fig. 2. Typical responses of a brisk-sustained (X) and a brisk-transient (Y) ganglion cell of the cat retina. *A*, response of a brisk-sustained (X) ON-centre unit to a light spot of 19′ diameter, 30 cd/m² brightness (background 13 cd/m²) and 5 sec duration projected into the receptive field centre. Middle trace spike recording, upper trace smoothed penrecorder output, lower trace timing of the light stimulus. The receptive field centre of the unit was 42′. *B*, response of a brisk-transient (Y) ON-centre unit at the same retinal location. The stimululus size in this case was 80′, the receptive field centre diameter 121′, other parameters as in *A*. *C*, antidromic response of the brisk-sustained (X) unit in *A* to electric stimulation of the optic tract. *D*, antidromic response of the brisk-transient (Y) unit in *B* to electric stimulation of the tract. The arrows indicate the stimulus artifacts, calibration bars, 2 msec, 1 mV, ten traces superimposed.

recorder trace of the response of a brisk-sustained (X) ON-centre unit to a light spot projected in its receptive field centre. The unit had a maintained activity of 30–40 spikes/sec and its light response after an initial transient component remained at a high sustained firing rate. This is clearly different from the brisk-transient (Y) ON-centre unit shown below (Text-fig. 2*B*). The maintained activity was 8–10 spikes/sec and the response decreased to a very low level after a strong initial transient component. The brisk-sustained (X) cell responded with a latency of 4·6 msec to electrical stimulation of the optic tract (Text-fig. 2*C*), the brisk-transient (Y) cell had a latency of 2·5 msec (Text-fig. 2*D*). In general the two classes of ganglion cells could be separated unequivocally by using the combination of the above mentioned tests.

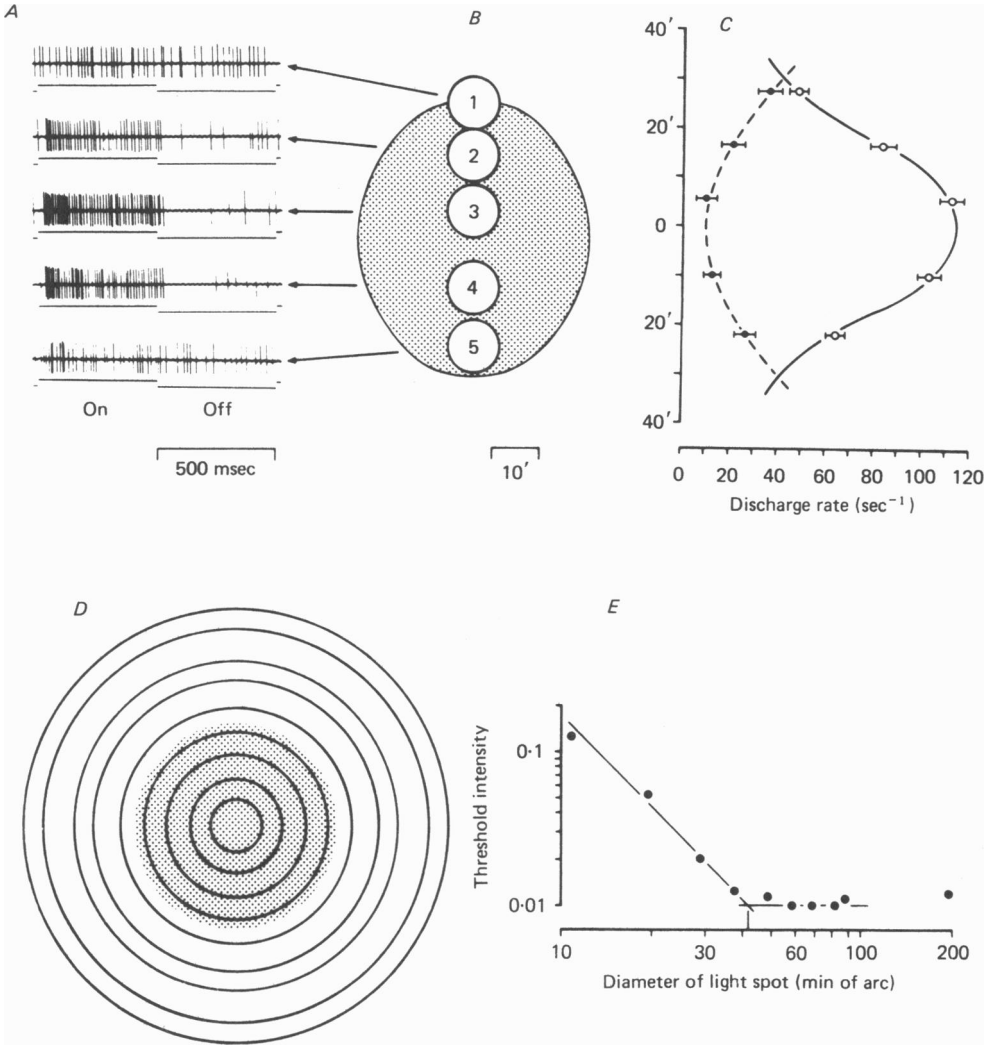

Text-fig. 3. Measurements of the receptive field centre of a brisk-sustained (X) ON-centre unit (same unit as Text-fig. 2 *A*, *C*). *A*, response of the unit to a light spot projected into different parts of the receptive field centre (spot diameter 11′, brightness 30 cd/m², background 13 cd/m², duration 500 msec). *B*, the stippled area indicates the receptive field centre, the stimulus positions (1–5) correspond to the recordings in *A*. *C*, average response of the cell to the light stimuli shown in the map *B*. Open circles (○), average response and standard deviation during light on for ten successive stimuli; filled circles (●), average response and standard deviation during light off. Continuous line, response profile of the ON-phase; broken line, response profile of the OFF-phase. *D*, map of the stimulus positions centred at the receptive field centre (stippled area) during the area-threshold measurements. *E*, area–threshold curve of this unit. The abscissa shows the diameter of the light disks in *D*, the ordinate is the threshold intensity necessary to elicit a centre type response. The axes are on logarithmic scale, ordinate scale relative.

2. *Receptive field centre diameters*

The first method of assessing the receptive field centre dimensions was an exploration with a small light spot which flashed on and off. Text-fig. 3*B* shows five successive positions of such an exploring spot in the receptive field centre (stippled area) of a brisk-sustained (X) ON-centre unit. When the spot was positioned in the centre (see Text-fig. 3*A*), the cell vigorously discharged during light on and the discharge rate was suppressed during light off. When the spot approached the border of the receptive field centre, the response at light on decreased and the suppression at light off also became weaker. At stimulus position 1 we could just hear a response of the cell at light on and this indicates the border of the receptive field centre by the acoustical discrimination method. The vertical extent of the receptive field centre assessed in that way was 56′, the horizontal extent 47′. This gives a ratio of short to long axis being 1·2 and a geometric mean of 51′ for the centre.

In order to determine the measurement errors introduced by the acoustical estimation of receptive field centre boundaries a quantitative evaluation of the cell's response during small spot mapping was carried out. The average response of this unit to stimulation at the five positions within the receptive field centre is shown in Text-fig. 3*C*. At position 1 the discharge rate was 48 ± 4 spikes/sec for the ON phase and 36 ± 5 spikes for the OFF phase, which is significantly different. Therefore the centre extends beyond that position. Bell-shaped curves, which describe the receptive field response profile of that cell, were fitted by eye to the on and off discharges. At the intersection of those two curves the discharges at light on and off no longer differ and this represents the border of the receptive field centre. On these criteria the vertical extent of the receptive field centre in Text-fig. 3*B* was 62′. This shows that assessing the borderline by ear results in an underestimation of the centre dimensions by about 10%.

The second method of assessing the receptive field centre dimensions was the area-threshold method (Barlow, Fitzhugh & Kuffler, 1957; Wiesel, 1960; Cleland & Enroth-Cugell, 1968), where the threshold of the cell for successively larger light spots (Text-fig. 3*D* and *E*) is measured. Text-fig. 3*E* shows on double logarithmic scale the decrease of the threshold intensity with increasing diameter of the light spots. By convention this curve is evaluated by two lines (Cleland & Enroth-Cugell, 1968; Cleland *et al.* 1973): A line of negative slope through the points at small diameters and a horizontal line through the points at the minimum threshold. Their intersection indicates the 'equivalent centre diameter', which for this particular cell was 42′. If one takes the minimum of the area-threshold curve in Text-fig. 3*E* which indicates the over-all size of the centre summating region of the cell, one ends up with $\sim$ 60′ centre diameter which is a factor 1·5 larger than the equivalent centre diameter.

The theoretical basis of this method was tested by calculating the area–threshold curve for an idealized receptive field. As proposed by Rodieck & Stone (1965) the sensitivity profile of a ganglion cell receptive field can be idealized by two Gaussian functions as shown in Text-fig. 4*A*. In the linear model the ganglion cell's response can be calculated by a convolution of the light distribution with this sensitivity profile. This was done numerically for disks of increasing diameters using the profile

of Text-fig. 4*A*. The intensity of those disks was variable and adjusted in the calculations to yield a constant threshold response of the cell. The result of the calculations is shown on double logarithmic scale in Text-fig. 4*B*. For small disks this area threshold curve can be approximated by a straight line of $-0{\cdot}8$ slope. The curve has

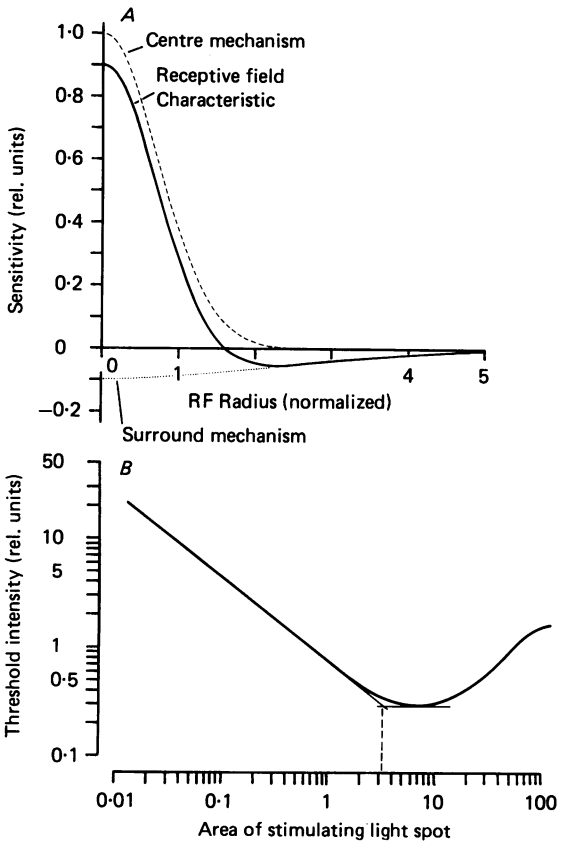

Text-fig. 4. Area threshold curve of an idealized receptive field. *A*, sensitivity profiles of the centre mechanism (dashed line), the surround mechanism (dotted line) and the over-all receptive field characteristic (continuous line), which is the linear sum of the centre and surround mechanism. Centre and surround mechanisms are Gaussian, the 1/e radius of the surround mechanism is three times that of the centre, the maximum sensitivity of the surround is 1/10 of the centre sensitivity. *B*, area threshold curve of the receptive field characteristic in *A*. This was calculated numerically, assuming linear summation. For spot areas between 0·01 and 1 the curve can be approximated by a straight line of slope $-0{\cdot}8$.

a clear minimum, where the strength of the centre mechanism in Text-fig. 4*A* is equal to that of the surround mechanism. For even larger disks the inhibitory action of the surround has the result of a threshold increase by about half a log unit. The line with $-0{\cdot}8$ slope intersects the horizontal line through the minimum at a disk area of 3·25 indicating an 'equivalent centre' radius of 1·02. This corresponds very closely to the radius 1·0, where in Text-fig. 4*A* the sensitivity of the centre mechanism has dropped to 1/e, which is 37 % of its maximum value. The minimum of the

area threshold curve in Text-fig. 4*B* is found at an area of 8·0, indicating a radius of 1·6. This is exactly the radius, where in the sensitivity profile of Text-fig. 4*A* the receptive field characteristic intersects the zero ordinate, and where the centre mechanism has dropped to $\simeq 1/10$ of its maximum value. The equivalent centre

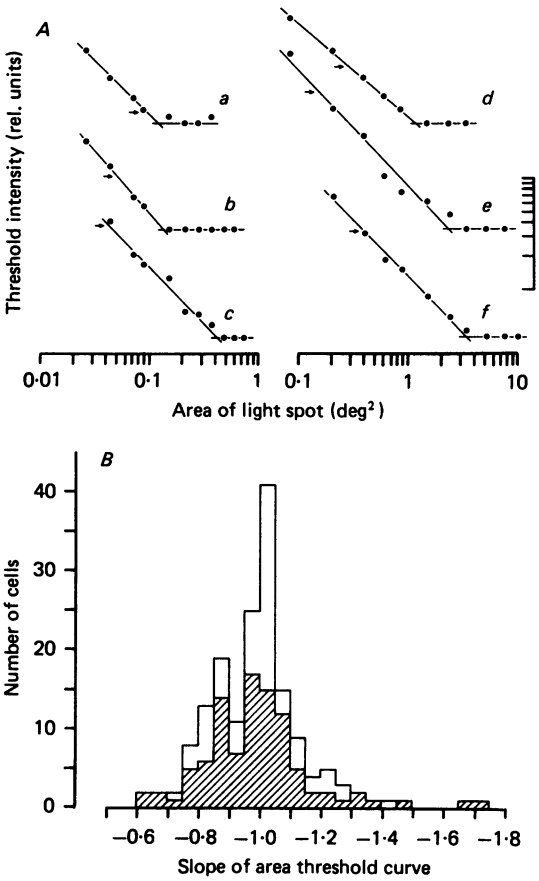

Text-fig. 5. *A*, some typical area threshold curves of brisk-sustained (X) (*a–c*) and brisk-transient (Y) cells (*d–f*). The ordinates are shifted arbitrarily to separate the curves, but can be recalibrated (scale on the right) by means of the arrows, which indicate a light intensity of 27·7 cd/m² for each of the curves (background 13 cd/m²). *B*, histogram of the slopes measured in the area–threshold curves. The hatched area indicates brisk-transient (Y) units, the unstructured area brisk-sustained (X) cells. $n = 166$; mean = −0·99; S.D. = 0·16. □, 97, −0·99, 0·18; ▨, 69, −0·99, 0·13.

diameter therefore is an underestimate of the centre dimensions by a factor of about 0·64, which is in accordance with the experimental evidence presented above (Text-fig. 3*E*).

If the sensitivity profile of the receptive field centre has a Gaussian form, the slope of the area threshold curve for small disks is −0·8 (Text-fig. 4*B*). A line of the slope −1 drawn through the points at smaller diameters to intersect a second, horizontal line through the points near minimum threshold would represent the

behaviour of an idealized centre mechanism having a rectangular distribution of sensitivity. In such a distribution of sensitivity Ricco's law (area × intensity = constant) is valid. Text-fig. 5*A* shows some typical experimental area-threshold curves and their evaluation by a line of negative slope and a horizontal line to assess the equivalent centre diameters. Text-fig. 5*B* is a summary of the slopes we have measured in 166 area threshold curves. The mean slope was about -1, a result which is surprising after the theoretical considerations just presented, because this would

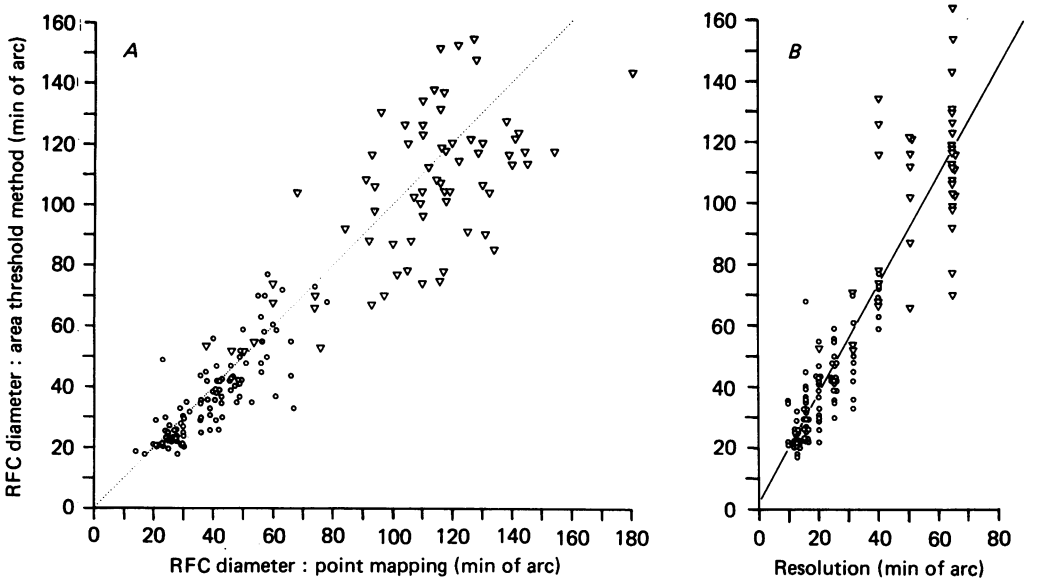

Text-fig. 6. Comparison of the three methods used to assess the receptive field centre dimensions. *A*, scatter diagram comparing small spot mapping with the area-threshold method. Each dot represents a single unit (○ brisk-sustained (X) cells, ▽ brisk-transient (Y) cells), the ordinate indicates the receptive field centre diameter of the unit according to the area-threshold method, the abscissa according to small spot mapping. The dotted line (slope $+1$) respresents exact correspondence. *B*, correlation between spatial resolution and equivalent centre diameter. The ordinate shows the centre diameter of a unit, the abscissa the period length of the moving grating, which could just be resolved (symbols as in *A*). Continuous line, linear regression.

mean that most sensitivity profiles are rectangular and non-Gaussian. In the discussion of this paper it will be shown that this deformation of the sensitivity profile from Gaussian to rectangular or even hyperbolic form (slopes even smaller than -1) could be due to the influence of the nonlinear gain of the receptors.

The third method for measuring the receptive field centres was to determine the upper limit of the spatial resolution of ganglion cells for moving square wave gratings. It has been shown by Wässle & Creutzfeldt (1973) for concentrically organized single units of the cat LGN that the resolution limit (the period length of the grating which is just resolved) is about half the diameter of the receptive field centre. Text-fig. 6*B* represents the resolution limit of the cells in a scatter diagram. The highest resolution was contributed by brisk-sustained (X) units of the central area and was in the range

of 10′ which corresponds to 6 cycles per degree. A linear regression line was calculated for the correlation between resolution and receptive field centre size. The slope of that line was 1·82, which is very close to the result of Wässle & Creutzfeldt (1973). Although the data exhibit a rather big scatter they are clustered along that line and the resolution limit is a linear function of the receptive field centre diameter.

In Text-fig. 6*A* the receptive field centre diameters of all units measured by small spot mapping and the area-threshold method are compared. If both sets of data always give the same estimation of centre diameters the points would exactly coincide with the dotted line of the slope +1. There is a slight indication that more units are below that line than above, which means that if one measures the receptive field centre of a unit with the area–threshold method one gets a smaller diameter than with the point mapping procedure. This is a confirmation of the theoretical considerations (Text-fig. 4) and of the result discussed in Text-fig. 3, where the 'equivalent centre diameter' was 42′ and the diameter assessed by small spot mapping was 51′.

Both in Text-fig. 6*A* and Text-fig. 6*B* there is substantial scatter of the receptive field dimensions assessed by the three methods, although their interdependence is clear. The reasons for the scatter might be due to non-circular fields, different sensitivity profiles, and fluctuations in the acoustical discrimination. The three methods are affected by those error sources in different and non-controllable ways. One therefore has to decide which method is the most reliable for the presentation of the results. This without any doubt is the area-threshold method. It is not affected by the subjective acoustical threshold, which only shifts the curve up or down, nor by the intensity and the size of the exploring spot nor by stray light. Moreover the final centre diameter is not the result of a single measurement but has been obtained by eight to ten independent threshold settings. Therefore for the rest of this paper specifications of receptive field centre dimensions always refer to equivalent centre diameters assessed by the area–threshold method.

3. *Variation of receptive field centres with eccentricity*

In Text-fig. 7*A* the receptive field centre dimensions of all 166 units are presented, pooled from all retinal locations according to their eccentricity. Brisk-sustained (X) cells increase their centre diameter from 20′ in the central area to about 70′ at 4·5 mm eccentricity. Brisk-transient (Y) cells have larger receptive field centres at all eccentricities, 50′ in the central area and about 140′ at 5 mm eccentricity. Both classes contain ON-centre and OFF-centre units; dimensional differences between those groupings could not be detected. For technical reasons (the recording apparatus could not be tilted further towards the temporal retina) we were not able to record from cell bodies with larger eccentricities. Occasionally we recorded the axons of ganglion cells positioned in the far temporal retina (eccentricity $\simeq$ 7–8 mm) and their receptive field centre sizes clearly exceeded those at 4 mm eccentricity. This agrees with the further increase of the centre sizes beyond 4 mm described by previous authors (Hammond, 1974; Stone & Fukuda, 1974).

There is a rather big scatter of centre sizes and especially between 1·5 and 2·5 mm eccentricity a complete range of receptive field centres from 30 to 120′ is found. This scatter could have been introduced as a result of pooling the data from different

animals and different topographical positions on the retina, which could blur the two primarily discrete groups of centre sizes. To test this we recorded in one cat, in a small region of the retina as many cells of either type as possible and measured their receptive field centres. Pl. 1, fig. 3 is the map of the cell positions on the external tangent screen; nine brisk-transient and thirteen brisk-sustained cells were analysed in a small region of the retina. At the end of the experiment an electrolytic lesion (asterisk Pl. 1, fig. 3) was made and identified in a whole mount of that retina. Pl. 1, fig. 1 is a low power micrograph of the whole mount. The outlined region corresponds

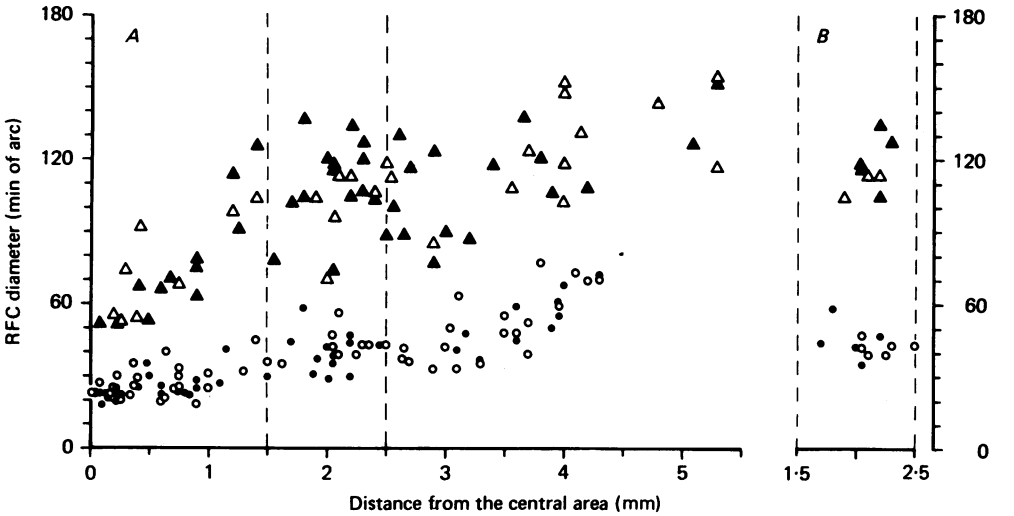

Text-fig. 7. Receptive field centre sizes as functions of eccentricity. *A*, the abscissa shows the eccentricity of a particular cell in mm on the retinal whole mount, corrected for screen distortions (○ brisk-sustained (X) ON-centre, ● brisk-sustained (X) OFF-centre, △ brisk-transient (Y) ON-centre, ▲ brisk-transient (Y) OFF-centre. The ordinate indicates the 'equivalent centre' diameters. For example in the eccentricity band 1·5–2·5 mm (indicated by the two dashed vertical lines) a rather complete range of centre sizes seems to exist. *B*, centre sizes of the critical band between 1·5 and 2·5 mm, all from one cat and a small retinal field. The topographical positions of those cells are shown in Pl. 1, fig. 3, the corresponding retinal whole mount in Pl. 1, fig. 1, 2.

to the recording area of Pl. 1, fig. 3, its distance from the central area was 1·5–2·5 mm towards the temporal retina. Pl. 1, fig. 2 is an enlarged photomirograph of that recording region. A comparison of the histological preparation (Pl. 1, fig. 2) with the map of the cells recorded from that region (Pl. 1, fig. 3) shows that of the several hundred ganglion cells present in that particular retinal location only some twenty could be recorded. Although the sample is small, it makes an important point: Text-fig. 7*B* shows the eccentricity and receptive field dimensions of those units. The brisk-sustained (X) cells have centre dimensions from 35 to 58′ (mean 44′), the brisk-transient (Y) cells from 104 to 134′ (mean 116′). This means that both populations are clearly separated. The 95% confidence limits for the centre size of brisk-sustained (X) cells in that area are 30·5–56·9′, those of the brisk transient (Y) cells 92–140·5′, thus the sample size is big enough to show the clear separation of centre sizes. Recording from one cat and one retinal location does not produce the scatter

of receptive field centre dimensions present in the same eccentricity range of Text-fig. 7*A*, which is therefore more apparent than real. Pooling from different cats, which have different eye size, different power of the dioptric apparatus of the eye and also differing sizes of the retina and the retinal landmarks (which were routinely assessed from the whole mounts) is an obvious source of the scatter of receptive field centre dimensions.

The influence of the retinal topography on the scatter is more interesting: Comparing the ganglion cell density of the top of Pl. 1, fig. 2 with that of the bottom one can notice an increase of ganglion cell density. The bottom of this figure touches the 'streak', the horizontal arm of higher ganglion cell density in the cat retina (Stone, 1965; Hughes, 1975). In the recordings illustrated in Pl. 1, fig. 3 we found a slight decrease of centre dimensions when approaching the streak, which indicates that in regions with higher ganglion cell density the receptive field centres are smaller. Therefore not only the eccentricity of a given cell has to be recorded but also its exact topographical location on the retina. Pooling from different locations according to eccentricity introduces a scatter of centre sizes. A similar interrelation between density and dendritic field size has been found for horizontal cells of the cat retina: along the streak the density is high and this is paralleled by small dendritic fields (Wässle, Peichl & Boycott, 1978).

4. *Coverage of the retina with ganglion cell receptive field centres*

At each retinal position the receptive field centres of several neighbouring ganglion cells overlap. By electro-physiological recordings it is not possible to answer the question how many ganglion cells cover each point of the retina in that way. As pointed out above, only a small proportion of the ganglion cells can be recorded in any one experiment. Moreover the recording probability of large cell bodies is higher than that of small ones and therefore the recording percentage does not agree with the actual percentage of cells (Cleland & Levick, 1974*a*, *b*). One therefore has to use histological methods, which stain all ganglion cells of the retina, in a region where the cell bodies of brisk-sustained (X) and brisk-transient (Y) cells can be recognized. It has explicitly been shown that the brisk-transient (Y) units are identical with the large cells of Nissl stained retinae (Cleland *et al.* 1975) which are the alpha cells in Golgi-stained retinae (Boycott & Wässle, 1974). There is only little doubt that brisk-sustained (X) cells are identical with the beta cells of Golgi-stained retinae (Boycott & Wässle, 1974; Cleland & Levick, 1974*a*, *b*; Stone & Fukuda, 1974), which have medium-sized cell bodies in Nissl-stained material. The remaining physiological classes of ganglion cells mainly have slow axonal conduction velocity and are thought to belong to the anatomical gamma class. In Nissl preparations those cells have small cell bodies. By using different staining methods (Gros-Schultze method, Bodian method and similar reduced silver stainings) we have developed procedures to stain quantitatively the cell bodies of the beta population and also to recognize them in Nissl-stained whole mounts. Details of this anatomical study are presented elsewhere (Wässle & Peichl, in preparation). A frame inside Pl. 1, fig. 2 marks the region, where by intensive recordings (see receptive field positions in Pl. 1, fig. 3) the centre sizes were well established. Text-fig. 8*A* shows a magnified drawing of the ganglion cell outlines from that region, which was done directly from the microscope by using

a Carl Zeiss drawing apparatus. The cells were classified according to the above-mentioned criteria into alpha, beta and gamma cells. The perikaryal area of those cells was measured and the resulting histogram is shown in Text-fig. 8*B*. The twelve alpha cells form the population of cells beyond 500 μm^2 perikaryal area, which means they have cell body diameters larger than 25 μm. The peak of the beta cell distribution is at about 260 μm^2, which means they have an average diameter of about 18 μm. The gamma cell peak occurs at about 100 μm^2 and their average diameter therefore is about 11 μm. The alpha cell population is clearly separated from the other two classes in that histogram. Beta and gamma cells overlap, but the above mentioned staining methods enabled us to separate the two populations also in the zone of overlap (Wässle & Peichl, in preparation). Thus of the 383 ganglion cells present in Text-fig. 8*A*, twelve were classified as alpha cells (3%), 211 were classified as beta cells (55%) and 160 as gamma cells (42%). The relative percentages of the three cells classes at that topographical position were also confirmed by different other staining methods. In the central area the percentages have shifted and relatively more beta cells are encountered: alpha 2%, beta 60–70% and gamma 30–40%. In the periphery of the retina one finds relatively more gamma cells: alpha 3–4%, beta 30–40%, gamma 60–70%. But in absolute numbers all three cell classes have their highest density in the central area.

Combining this histological result with the previously presented receptive field centre dimensions one can calculate the number of ganglion cells of each class overlapping at every point of that particular retinal field. The coverage factor is the product of cell density and area of the receptive field centre (Cleland *et al.* 1975). It is important that both sets of data were from the same retina, because this allows direct transformation of the receptive field centre dimensions, measured as visual angles on the tangent screen, into retinal dimensions on the whole mount. The retinal landmarks backprojected onto the external tangent screen and the position of the lesion could be recognized on the whole mount of the retina and it was calculated that 1° on the screen corresponded to 208 μm retinal distance. Errors, introduced by the shrinkage of the whole mount or by the additional optical power of the spectacle lens are thus ruled out. The alpha cell density in the recording area was 35/mm^2, the average receptive field centre diameter of brisk-transient (Y) cells was 0·40 mm (area 0·127 mm^2) and from that the coverage factor was calculated to be 4·4. For the brisk-sustained (X) class the density was 620/mm^2, the average receptive field centre diameter 0·15 mm (area 0·018 mm^2) and thus the coverage factor was 11·4.

In a similar retinal whole mount the densities of alpha and beta cells were measured along a line of intersect tilted 30° towards the upper temporal retina. The alpha cell density decreases from about 200/mm^2 in the central area to $\simeq$ 3 cells/mm^2 in the far periphery (Text-fig. 9*A*, filled triangles) and the beta cell density decreases from 6500/mm^2 in the central area to about 80/mm^2 in the far periphery (Text-fig. 9*B*, filled circles). The receptive field centre measurements of this paper (see Text-fig. 1) are symmetrically scattered around that line of intersect, which therefore yields a reasonable approximation of the cell densities at their actual topographical positions. The receptive field centres as derived from Text-fig. 7 are also inserted in Text-fig. 9*A* and *B*. They increase with distance from the central area. The coverage of the retina with brisk-transient (Y) units shown in Text-fig. 9*C* is rather constant over

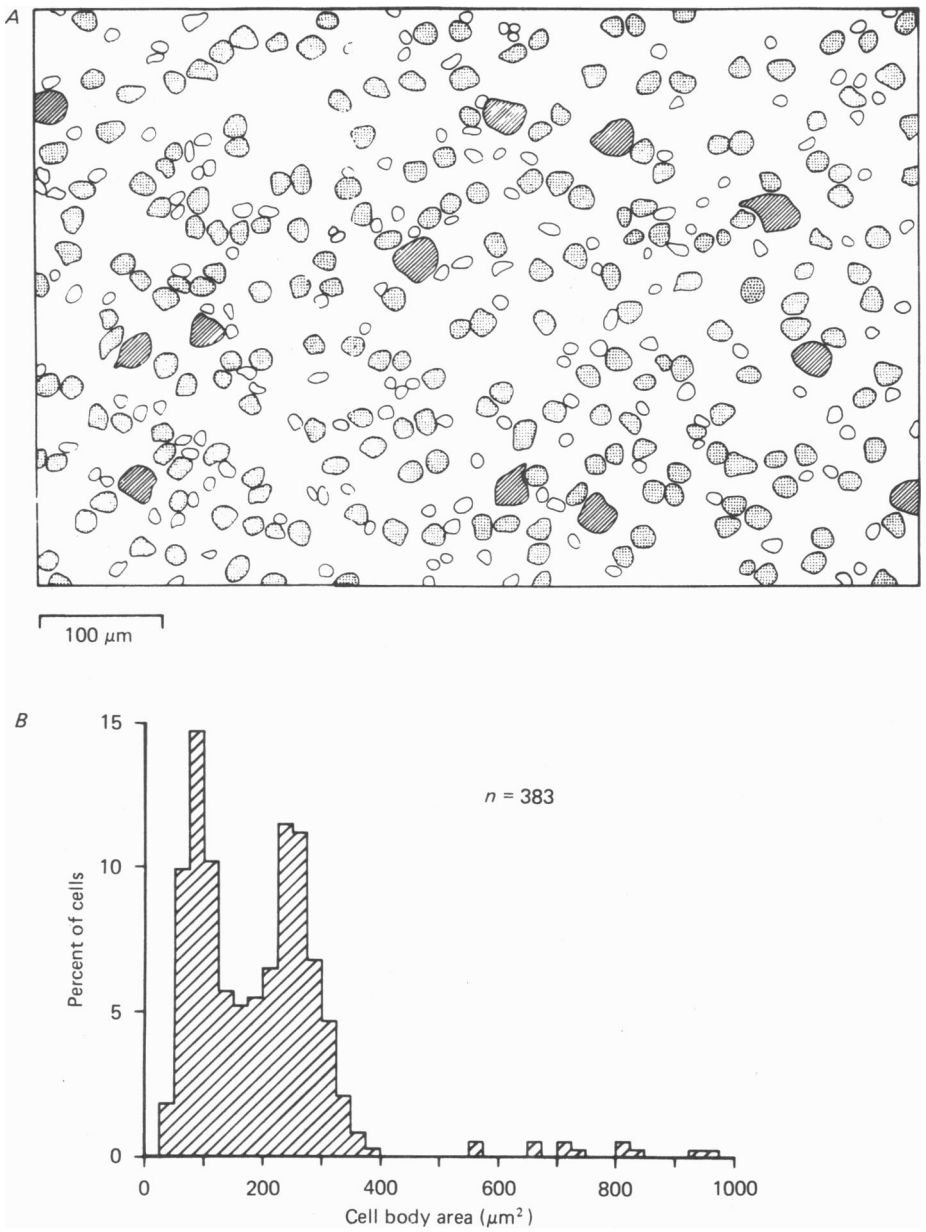

Text-fig. 8. Classification of ganglion cells from a Nissl-stained retinal whole mount. *A*, outlines of the ganglion cell bodies from the retinal area inside the frame of Pl. 1, fig. 2. Hatched somata were classified as alpha cells, dotted somata as beta cells, the small unlabelled somata belong to the Gamma population. *B*, histogram of the cell body areas of the ganglion cells shown in *A* (measured with a semi-automatic image analyser, Leitz A.S.M.). $n = 383$.

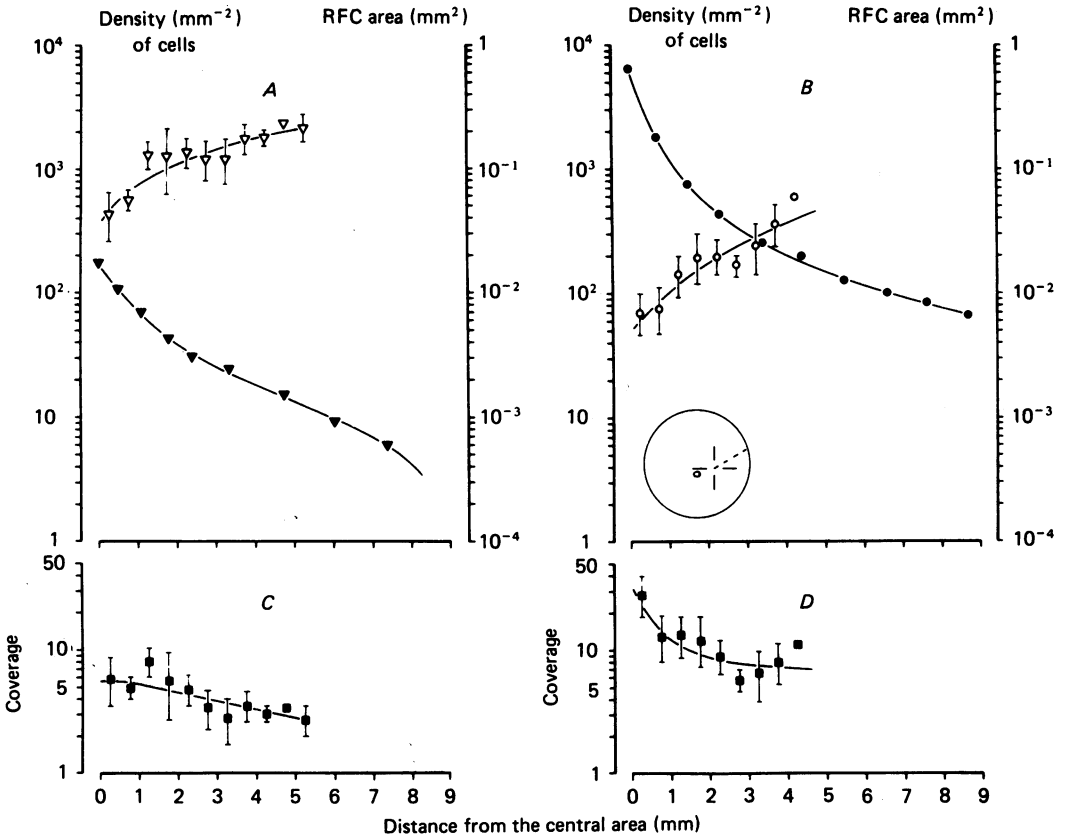

Text-fig. 9. Coverage of the retina with brisk-sustained (X) and brisk-transient (Y) cells. *A*, the abscissa shows the distance from the central area, the left ordinate the density of alpha cells (▼), the right ordinate shows the receptive field centre area of brisk-transient (Y) cells (▽), *B*, abscissa and ordinates as in *A*, filled circles (●) beta cell densities, open circles (○) receptive field centre area of brisk-sustained (X) cells. *C*, coverage of the retina with brisk-transient (Y) cells as a function of retinal eccentricity. *D*, coverage of the retina with brisk-sustained (X) cells as a function of retinal eccentricity. The inset in *B* indicates in a schematic map of the retina the line of intersect along which the alpha and beta densities were measured. All curves fitted by eye.

the retina between 3 and 5·5. Thus the big decrease of density between centre and periphery is balanced by a simultaneous increase of the receptive field dimensions, with the effect that each point of the retina is covered by at least three brisk-transient (Y) cells. The situation for the brisk-sustained (X) cells is different (Text-fig. 9*D*). For most of the retina their coverage factor is 7–10, but in the central area it increases up to 30. Yet in this class too, the rather steep ganglion cell density decrease from centre to periphery by a factor of 40 is partly balanced by a simultaneous increase of receptive field centre dimensions. It has to be emphasized that the above calculated 'coverage factors' were derived for 'equivalent centre sizes'. If one refers to the overall centre summating region, the coverage factor would be higher by a factor 2·25.

DISCUSSION

The size of the receptive field centre

Since Hartline (1938) introduced the term 'receptive field' for that part of the visual space where a single unit can be influenced by a light stimulus, this concept has been a major guideline of visual neurophysiology (Kuffler, 1973). The properties of a distinct part within the receptive field of a ganglion cell, the receptive field centre, essentially determine the role a ganglion cell might play in visual information processing. It has been shown in the present paper that the quantification of the receptive field centre dimensions critically depends upon the method used. Moreover each of those methods has shortcomings, which may be expected to influence the results. A comparison of the results presented in this study with those of previous authors has to be restricted to more recent papers where both the eccentricity and the type of the ganglion cells have been specified. Table 1 summarizes the dimensions presented

TABLE 1. Comparison of the receptive field centre dimensions of cat retinal ganglion cells presented by different authors

Ecc. ... / Source	Type	Central area	1 mm	2 mm	3 mm	4 mm	5 mm
		Diameter of the receptive field centre (min of arc)					
Stone & Fukuda (74)	X	10–12	15–30	20–50	20–55	40–65	45–70
	Y	30–40	45–85	55–140	75–135	70–145	75–140
Cleland & Levick (74)	b.s.	33	35–60	45–75	50–80	—	—
	b.t.	58–65	70–140	100–160	120–165	—	—
Hammond (74)	b.s.	—	55–110	55–160	55–165	55–140	65–145
	b.t.	—	105–150	105–160	115–190	125–190	125–200
this paper	b.s.	18–23	20–40	30–60	33–63	50–77	—
	b.t.	52	60–100	70–135	80–140	100–150	115–155
		Diameter of the dendritic tree (min of arc)					
Boycott & Wässle (74)	beta	6	10–25	15–35	20–50	25–60	30–65
	alpha	50	70–110	90–140	100–160	115–180	125–190

by the different authors, specified according to the type of ganglion cell and eccentricity. All authors agree that brisk-sustained (X) cells have smaller receptive field centres than brisk-transient (Y) cells, and all authors find an increase of the centre dimensions with increasing distance from the central area. But there are remarkable differences in detail. The smallest X cells in the central area are 10–12′ according to Stone & Fukuda (1974) while Cleland & Levick (1974*a*) find 33′ for those cells. Our result of 18–23′ lies between these. To understand such large differences, the methods used for receptive field measurements and their limitations have to be discussed.

The small spot mapping is applied in two versions. In the 'elaborate' version a small light spot of constant intensity is positioned in different parts of the receptive field and the response of the cell is evaluated by spike counting. This method gives precise information about the response profile of the cell (Text-fig. 3*B* and *C*) and has

been described in detail by Rodieck & Stone (1965). For routine measurements of receptive field sizes it is too complicated and a 'reduced' version is used, in which the border of the receptive field centre is defined by subjective acoustical discrimination. In this form it was used by Cleland & Levick (1974*a*, *b*), Hammond (1974), Stone & Fukuda (1974) and also in this paper. If in this method the exploring spot is chosen too large one obtains larger receptive fields, if the spot is too bright, the stray light also tends to enlarge the centre. On the other hand the subjective acoustical discrimination requires a clear response and therefore tends to decrease the centre size. For those reasons we have applied this method for comparison only.

The explanation why Stone & Fukuda (1974) got smaller receptive field centres might be found in the method they used. Their 1974 paper does not describe the method, but instead refers to the earlier paper of Hoffmann, Stone & Sherman (1972), where one reads: 'To plot each of the smallest centre regions, which were only slightly bigger than the smallest test spot, we first located the position of the centre region. We then sequentially moved the test spot, flashing at about 2 Hz, towards the centre region from positions above, below, to the left of, and to the right of the centre until a weak centre response was first elicited. The spot was held at this position and the edge of the spot closest to the receptive field centre was marked.' They used a *weak* response and they made a mark at *the edge* of the spot, not at its centre. Therefore, their marks underestimate the diameter of the centre by twice the radius of the spot being used.

Our data agree very well with the results obtained by Cleland & Levick (1974*a*), except for the centre of the central area. They assessed the central area only by back-projecting the retinal landmarks onto the external tangent screen. We routinely checked the backprojections by histology and found the backprojected estimations of the central area only accurate within about 2° of visual angle. It therefore might be that Cleland & Levick (1974) have not recorded cells from the exact centre of the central area, thus missing the smallest fields.

Hammond (1974) only specifies the long axes of the receptive fields, therefore the centre sizes he presents are larger than those of all other authors.

The area threshold method avoids most of the difficulties mentioned above, in particular it is robust against the subjective acoustical discrimination method. If an experimenter's threshold is consistently higher, the whole area-threshold curve will shift to higher light levels, but the overall shape of the curve will not be changed. However the method also has disadvantages, for precise centring of all light spots is crucial. Furthermore elliptical receptive fields create problems: The receptive fields measured by the small spot mapping were oval, the mean ratio long axis/short axis was 1·14 ($\pm$ 0·13). Therefore for circular light stimuli there is a *prima facie* case of an error as large as 14%. Additionally for Gaussian sensitivity profiles the equivalent centre diameter is an underestimate of the centre summating region by a factor of 0·66.

We also showed for a Gaussian sensitivity profile and linear summation that the initial part of the area–threshold curve can be approximated by a line of the slope $-0{\cdot}8$. In the actual measurement we found in agreement with previous authors (Barlow *et al.* 1957; Cleland *et al.* 1973; Enroth-Cugell, Hertz & Lennie, 1977) an average slope of -1 indicating a rectangular sensitivity profile and Ricco sum-

mation. The reason for this discrepancy might be found in the non-linear transfer of the receptors, which can be approximated by a hyperbolic function (Naka & Rushton, 1967). The Gaussian sensitivity profile normally is measured as the response of the ganglion cell to a small light spot of *constant* light intensity, which is projected into different parts of the receptive field. Thus the receptor output is kept constant and it is mainly the ganglion cell characteristic which is tested. This is not so in area threshold measurements; the smallest light spot usually is more than one log unit brighter than the large spots of low intensities (Text-fig. 4*A*). The bright small spots are more attenuated by the non-linear receptor transfer than the dim large spots. To yield a suprathreshold effect on the ganglion cell level they have to be brighter than predicted by the linear model. Therefore the area–threshold curves are shifted to higher light intensities in the small spot region and have a slope steeper than $-0{\cdot}8$.

The area threshold curves of brisk-sustained (X) units presented in this paper (Text-figs. 3*E* and 5*A*) did not bend up at large spot sizes as did those presented by Cleland *et al.* (1973). We were aware of this difference during the experiments and carefully determined the threshold for large spots, but could not find this threshold elevation by as much as one log unit. It might be that the higher repetition rate of the light stimuli used in the present experiments (1 Hz compared with 0·5 Hz used by Cleland *et al.* 1973) has changed the temporal course of the response and has caused a different threshold criterion for large spots (Barlow & Levick, 1969). The rather low light level in use may also have been a factor.

The anatomical basis of the receptive field centre

The anatomical basis of the receptive field centre was thought to be the dendritic field of retinal ganglion cells (see Levick, 1975, as a summary). A direct correlation of the receptive field measurements presented in this paper with the dendritic field measurements of Boycott & Wässle (1974) has to account for two factors: the first is the conversion of the receptive field data, which are measured in visual angle, into retinal distance. This conversion was achieved in the present paper by constructing whole mounts of the retina, where a defined lesion and the retinal landmarks could be correlated with their backprojected images on the tangent screen. The other factor is the shrinkage of Golgi preparations, which was not corrected by Boycott & Wässle (1974). Recent anatomical studies from comparable material (Wässle, Boycott & Peichl, 1978) have shown that the Golgi whole mounts of Boycott & Wässle (1974) were shrunk in area by a factor of about 0·6, therefore underestimating the linear dimensions by about 0·77. The equivalent centre diameters are an underestimation of the actual receptive field centres by about 0·66 and should therefore directly be comparable with the dendritic field dimensions of Boycott & Wässle's Golgi data not corrected for shrinkage.

The brisk-sustained (X) cells of Text-fig. 8*B* had equivalent centre dimensions between 121 and 201 μm (mean 152 μm), the brisk-transient (Y) cells between 360 and 464 μm (mean 402 μm). For the same retinal eccentricity Boycott & Wässle (1974) described the range of beta cell dendritic field diameters as being 60–120 μm and the range of alpha cell dendritic fields as being 320–500 μm. Thus the dimensions of alpha and brisk-transient (Y) cells agree very well but the brisk-sustained (X) cells

have significantly larger dimensions than the beta cells. This is the case for all other eccentricities too, as can be seen from Table 1, where the dendritic field dimensions (lowest line) are compared with the receptive field centre measurements. An error in the estimation of the shrinkage factor of the Golgi whole mount preparations can not be the explanation for this difference, because the ratio of alpha dimensions to beta dimensions should then agree with the ratio of the corresponding receptive field centre dimensions. But it does not, being about 4 in the histology compared with 2·6 in the physiology. Two other reasons might explain that difference. It could be that the beta cell population is understained and therefore their dendritic fields might be underestimated. Such a possibility cannot be ruled out, because alpha cells have rather thick dendrites, which are more safely stained than the delicate branches of beta cells. It is also known (Boycott, Peichl & Wässle, 1978) that the Golgi-Cox method sometimes does not stain the finest branches of nerve cells, and most of the dendritic field measurements of Boycott & Wässle (1974) were from Golgi-Cox stained material. A second reason for the larger receptive fields of brisk-sustained (X) cells might be deduced from the retinal wiring. The ganglion cells are not directly connected with the receptors, but three layers of neurons (horizontal, bipolar, amacrine cells) are found in between, all having dendritic fields which might add to the spatial extent of the ganglion cell dendritic tree to form the receptive field centre dimensions. The present data show that this expansion differs for brisk-sustained (X) and brisk-transient (Y) cells, suggesting a different retinal wiring for the construction of their receptive field centres. The lack of correspondence of the beta cell dendritic fields with the brisk-sustained (X) cell receptive field centres cannot mean that those two cell classes are not congruent, because there is no other cell class in the retina whose dendritic trees are small enough to match those receptive field centres.

Scatter of receptive field centres and spatial frequency transfer

Brisk-sustained (X) cells probably are the class of retinal ganglion cells important for resolution of fine detail and pattern analysis. Their small receptive fields and their high percentage in the central area support this idea. Campbell *et al.* (1969) and Graham, Robson & Nachmias (1978) have postulated that every point of the visual field is analysed by a set of channels covering a rather broad range of spatial frequency tuning curves. The question, on which level of the visual system (retina, l.g.n., visual cortex) those channels might be found physiologically can be discussed now. At each point of the retina only a minute scatter of the receptive field centre sizes of brisk-sustained (X) cells was found. Therefore the tuning curves are homogeneous, which does not meet the idea of a broad range of channels. Cleland *et al.* (1971) have measured the convergence of retinal ganglion cells onto single relay neurons of the lateral geniculate nucleus (l.g.n.). They found that each relay cell of the l.g.n. receives excitatory input from 3 ± 2 retinal ganglion cells. Because the receptive centres of those ganglion cells were found to overlap strongly, the receptive field centre of the geniculate unit was not much larger than that of a single retinal ganglion cell. Thus there is no evidence for a broad range of channels at each location of the retinotopic map in the geniculate. The earliest level where information processing by a broad range of sharply tuned spatial frequency channels might occur is the

visual cortex. Albus (1975) has shown that such a corresponding scatter of receptive field sizes actually exists in area 17 of the cat visual cortex.

An alternative way of achieving a rather broad range of spatial frequency tuning curves at every point of the visual field would be the convergence of signals from different physiological classes of retinal ganglion cells: Brisk and sluggish concentrically organized ganglion cells taken together cover a broad range of spatial frequency tuning curves. But it is still unclear how they interact in visual information processing.

Coverage of the retina by brisk-transient (Y) cells

At any point of the retina the receptive field centres of several ganglion cells overlap and therefore a multiple map of the visual world is transferred on to higher centres. The number of receptive field centres overlapping at a particular point, the so called coverage factor is the product of the density and the receptive field centre area of a given class of ganglion cell. Fischer (1973) calculated the coverage factor by using an average receptive field centre size and Stone's (1965) density data. He found the coverage to be 35 and constant over the whole retina. The pooling of the receptive field centre sizes independent of the physiological class of ganglion cell and the then unknown percentages of the individual classes have invalidated Fischer's (1973) estimate. Cleland *et al.* (1975) estimated the visual field coverage by brisk-transient (Y) receptive field centres and have found a coverage factor between 3 and 6, which agrees very well with our result. At first sight this multiple coverage seems to be redundant, but one has to keep in mind that a duplicate coverage is necessary for the representation of ON and OFF centre cells. Moreover there is a multiple projection of those units to the l.g.n., the m.i.n., the pulvinar and the superior colliculus, which would be facilitated by a multiple set of those ganglion cells.

Coverage of the retina by brisk-sustained (X) cells and spatial resolution

Two primarily independent parameters limit the spatial resolution of brisk-sustained (X) cells: The first is the spacing between neighbouring ganglion cells, known as 'sampling distance' (Barlow, 1964; Snyder & Miller, 1977), which can be calculated from the density of those cells. The second is the receptive field centre diameter of the cells, which acts as a 'sampling aperture' (Wässle & Creutzfeldt, 1973).

In the central area we found a beta cell density of 6500/mm^2 which includes equal numbers of ON and OFF centre brisk-sustained (X) cells. As long as we have no information about interaction of ON and OFF cells at higher visual centres we have to treat them as independent systems, which reduces the sampling densities (D) to 3250/mm^2 in each system. The corresponding intercellular distance (a) of a hexagonal array would be $a = (2/D.\sqrt{3})^{1/2} = 19\,\mu$m and the resolution limit (λ) would be $\lambda = a.\sqrt{3} = 33\,\mu$m (corresponding to 10′ or 6 cycles per degree). This resolution limit of 33 μm can only be achieved if the receptive field centres, the sampling apertures, do not exceed twice that value (Text-fig. 6*B*), which is 66 μm. From the density being 3250/mm^2 and this postulated 66 μm receptive field centre size a coverage of 11 is necessary to achieve the theoretical resolution limit. Thus for ON and OFF centre cells together the total coverage should be 22. Only brisk-sustained (X) cells

in the central area (see Text-fig. 9*D*) have a coverage larger than 22 and therefore meet the requirements of optimum resolution.

Coverage of the retina by sluggish-concentric and non-concentric ganglion cells

During the extensive exploration of the retina illustrated in Pl. 1 also a few sluggish and non-concentric cells (Cleland & Levick, 1974*a*, *b*) were encountered. Their receptive field sizes were in the range of the brisk-transient (Y) cells (0·13 mm^2). The density of the gamma class at that region was 470/mm^2 which would mean that those cells have a coverage factor as great as 60. This is not surprising if one keeps in mind that this group of cells might consist of nine separate classes (Cleland & Levick, 1974*b*). It is evident that each of those classes has a chance to cover each and every point of the retina several times. One therefore has to beware of concluding from the fact that a cell class is rarely encountered with the micro-electrode that it might not cover all retinal positions. This seems especially relevant for the colour specific ganglion cells; they are rare, but from the above number it is clear that each retinal point could be analysed by different colour channels.

This study was supported by a research grant of the Deutsche Forschungsgemeinschaft. We are grateful to B. B. Boycott, R. B. Freeman, Jr. and W. R. Levick for helpful discussion and comments. W. Skrandies helped with some of the experiments.

REFERENCES

ALBUS, K. (1975). A quantitative study of the projection area of the central and paracentral visual field in area 17 of the cat. I. The precision of the topography. *Expl Brain Res.* **24**, 159–180.

BARLOW, H. B. (1964). The physical limits of visual discrimination. In *Photophysiology*, vol. 2, ed. GIESE, A. C., pp. 163–202. New York: Academic.

BARLOW, H. B., FITZHUGH, R. & KUFFLER, S. W. (1957). Change of organisation in the receptive fields of cat's retina during dark adaptation. *J. Physiol.* **139**, 338–354.

BARLOW, H. B. & LEVICK, W. R. (1969). Three factors limiting the reliable detection of light by retinal ganglion cells of the cat. *J. Physiol.* **200**, 1–24.

BOYCOTT, B. B., PEICHL, L. & WÄSSLE, H. (1978). Morphological types of horizontal cell in the retina of the domestic cat. *Proc. R. Soc.* B **203**, 229–245.

BOYCOTT, B. B. & WÄSSLE, H. (1974). The morphological types of ganglion cells of the domestic cat's retina. *J. Physiol.* **240**, 397–419.

BROWN, J. E. & MAJOR, D. (1966). Cat retinal ganglion cell dendritic fields. *Expl Neurol.* **15**, 70–78.

CAMPBELL, F. W., COOPER, G. F. & ENROTH-CUGELL, C. (1969). The spatial selectivity of the visual cells of the cat. *J. Physiol.* **203**, 223–235.

CLELAND, B. G., DUBIN, M. W. & LEVICK, W. R. (1971). Sustained and transient neurones in the cat's retina and lateral geniculate nucleus. *J. Physiol.* **217**, 473–496.

CLELAND, B. G. & ENROTH-CUGELL, C. (1968). Quantitative aspects of sensitivity and summation in the cat retina. *J. Physiol.* **198**, 17–38.

CLELAND, B. G. & LEVICK, W. R. (1974*a*). Brisk and sluggish concentrically organized ganglion cells in the cat's retina. *J. Physiol.* **240**, 421–456.

CLELAND, B. G. & LEVICK, W. R. (1974*b*). Properties of rarely encountered types of ganglion cells in the cat's retina and an overall classification. *J. Physiol.* **240**, 457–492.

CLELAND, B. G., LEVICK, W. R. & SANDERSON, K. J. (1973). Properties of sustained and transient ganglion cells in the cat retina. *J. Physiol.* **228**, 649–680.

CLELAND, B. G., LEVICK, W. R. & WÄSSLE, H. (1975). Physiological identification of a morphological class of cat retinal ganglion cells. *J. Physiol.* **248**, 151–171.

CREUTZFELDT, O. D., SAKMANN, B., SCHEICH, H. & KORN, A. (1970). Sensitivity distribution and spatial summation within receptive field center of retinal on-center ganglion cells and transfer function of the retina. *J. Neurophysiol.* **33**, 654–671.

DOWLING, J. E. & BOYCOTT, B. B. (1966). Organization of the primate retina: electron microscopy. *Proc. R. Soc.* B **166**, 80–111.

ENROTH-CUGELL, C., HERTZ, B. G. & LENNIE, P. (1977). Convergence of rod and cone signals in the cat's retina. *J. Physiol.* **269**, 297–318.

ENROTH-CUGELL, C. & ROBSON, J. G. (1966). The contrast sensitivity of retinal ganglion cells of the cat. *J. Physiol.* **187**, 517–552.

FERNALD, R. & CHASE, R. (1971). An improved method for plotting retinal landmarks and focusing the eyes. *Vision Res.* **11**, 95–96.

FISCHER, B. (1973). Overlap of receptive field centers and representation of the visual field in the cat's optic tract. *Vision Res.* **13**, 2113–2120.

FISCHER, B., KRÜGER, J. & DROLL, W. (1975). Quantitative aspects of the shift-effect in cat retinal ganglion cells. *Brain Res.* **83**, 391–403.

GALLEGO, A. (1965). Connexions transversales au niveau des couches plexiformes de la rétine. *Actual. neurophysiol.* 6e sér., pp. 5–27, Paris: Masson et Cie.

GRAHAM, N., ROBSON, J. G. & NACHMIAS, J. (1978). Grating summation in fovea and periphery. *Vision Res.* **18**, 815–825.

HAMMOND, P. (1974). Cat retinal ganglion cells: size and shape of receptive field centres. *J. Physiol.* **242**, 99–118.

HARTLINE, H. K. (1938). The response of single optic nerve fibers of the vertebrate eye to illumination of the retina. *Am. J. Physiol.* **121**, 400–415.

HOFFMANN, K. P., STONE, J. & MURRAY SHERMAN, S. (1972). Relay of receptive field properties in dorsal lateral geniculate nucleus of the cat. *J. Neurophysiol.* **35**, 518–531.

HUGHES, A. (1975). A quantitative analysis of the cat retinal ganglion cell topography. *J. comp. Neurol.* **163**, 107–128.

KUFFLER, S. W. (1953). Discharge patterns and functional organization of mammalian retina. *J. Neurophysiol.* **16**, 37–68.

KUFFLER, S. W. (1973). The single-cell approach in the visual system and the study of receptive fields. *Investve Ophth.* **12**, 794–813.

LEVICK, W. R. (1972). Another tungsten microelectrode. *Med. Electron & biol. Engng* **10**, 510–515.

LEVICK, W. R. (1975). Form and function of cat retinal ganglion cells. *Nature, Lond.* **254**, 659–662.

LEVICK, W. R., OYSTER, C. W. & DAVIS, D. L. (1965). Evidence that McIlwain's periphery effect is not a stray light artifact. *J. Neurophysiol.* **28**, 555–559.

MCILWAIN, J. T. (1964). Receptive fields of optic tract axons and lateral geniculate cells: peripheral extent and barbiturate sensitivity. *J. Neurophysiol.* **27**, 1154–1173.

NAKA, K. I. & RUSHTON, W. A. H. (1967). The generation and spread of S-potentials in fish (cyprinidae). *J. Physiol.* **192**, 437–461.

RODIECK, R. W. & STONE, J. (1965). Analysis of receptive fields of cat retinal ganglion cells. *J. Neurophysiol.* **28**, 833–849.

SNYDER, A. W. & MILLER, W. H. (1977). Photoreceptor diameter and spacing for highest resolving power. *J. opt. Soc. Am.* **67**, 696–698.

STONE, J. (1965). A quantitative analysis of the distribution of ganglion cells in the cat's retina. *J. comp. Neurol.* **124**, 337–352.

STONE, J. & FUKUDA, Y. (1974). Properties of cat retinal ganglion cells: a comparison of W-cells with X-cells and Y-cells. *J. Neurophysiol.* **37**, 722–748.

STONE, J. & HOFFMANN, K. P. (1972). Very slow-conducting ganglion cells in the cat's retina: a major, new functional type? *Brain Res.* **43**, 610–616.

VENES, J. L., COLLINS, W. F. & TAUB, A. (1971). Nitrous oxide: an anesthetic for experiments in cats. *Am. J. Physiol.* **220**, 2028–2031.

WÄSSLE, H. (1975). A stereotaxic headholder for visual neurophysiology. *Expl Brain Res.* **23**, 151–156.

WÄSSLE, H., BOYCOTT, B. B. & PEICHL, L. (1978). Receptor contacts of horizontal cells in the retina of the domestic cat. *Proc. R. Soc.* B **203**, 247–267.

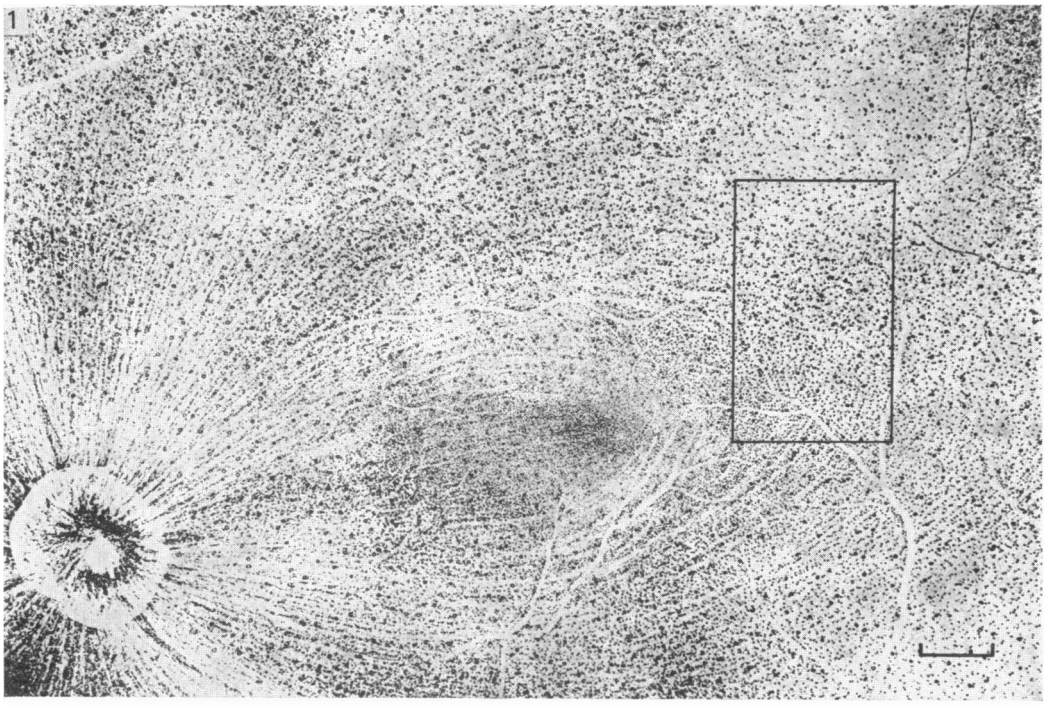
1

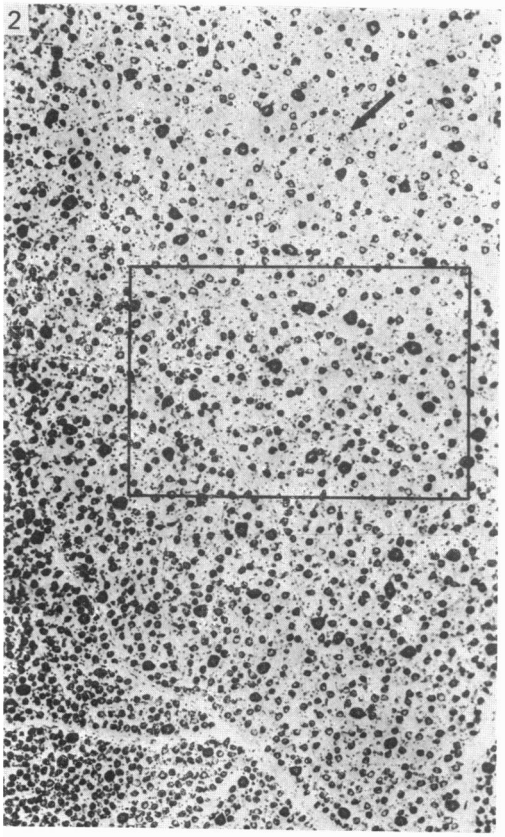
2

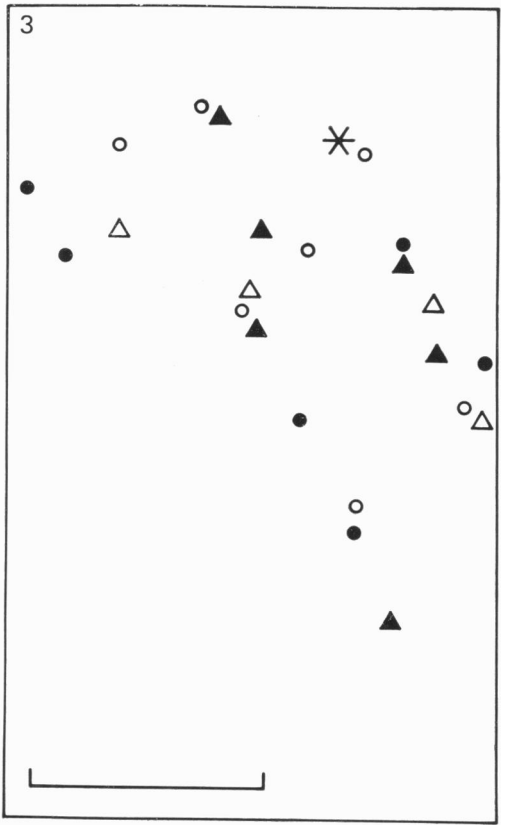
3

WÄSSLE, H. & CREUTZFELDT, O. D. (1973). Spatial resolution in visual system: a theoretical and experimental study on single units in the cat's lateral geniculate body. *J. Neurophysiol.* **36**, 13–27.

WÄSSLE, H., LEVICK, W. R. & CLELAND, B. G. (1975). The distribution of the alpha type of ganglion cells in the cat's retina. *J. comp. Neurol.* **159**, 419–438.

WÄSSLE, H., PEICHL, L. & BOYCOTT, B. B. (1978). Topography of horizontal cells in the retina of the domestic cat. *Proc. R. Soc.* B **203**, 269–291.

WIESEL, T. N. (1960). Receptive fields of ganglion cells in the cat's retina. *J. Physiol.* **153**, 583–594.

EXPLANATION OF PLATE

Fig. 1, low power micrograph (montage). Cresyl-violet-stained whole mount of the retina, where the scatter of receptive field sizes at one retinal location was tested. The optic nerve head is visible in the lower left corner, the convergence of blood vessels and the high ganglion cell density indicate the central area in the middle of the micrograph. The distance from the optic nerve head centre to the central area is 3·46 mm. The frame indicates the position of the magnified micrograph in fig. 2. Fig. 2, region of the whole mount, where the recordings were performed. The arrow indicates the lesion, which could clearly be recognized under higher power. The frame shows the area from which the magnified plot in Text-fig 8*A* was taken to classify the cells. Fig. 3, locations of the units which were recorded during that particular experiment. The scale and frame of that plot was adjusted to coincide with the micrograph in fig. 2. The asterisk indicates the position where the lesion was made. Other symbols as in Text-fig. 7.